Synthetic and Structural Studies of Butterfly Fe/S/P Cluster Complexes Related to the Active Site of [FeFe]-Hydrogenases. Proton Reduction to H_2 Catalyzed by $(\eta^1\text{-}Ph_2PS\text{-}\eta^1)_2Fe_2(CO)_6$

Li-Cheng Song,* Guang-Huai Zeng, Shao-Xia Lou, Hui-Ning Zan, Jiang-Bo Ming, and Qing-Mei Hu

Department of Chemistry, State Key Laboratory of Elemento-Organic Chemistry, Nankai University, Tianjin 300071, People's Republic of China

Received January 29, 2008

The butterfly Fe/S cluster anions $(\mu\text{-RS})(\mu\text{-S}^-)Fe_2(CO)_6$ (**A**, R = Et, *p*-MeC_6H_4), $(\mu\text{-S}^-)_2Fe_2(CO)_6$ (**C**), $[(\mu\text{-S}^-)Fe_2(CO)_6]_2(4\text{-}\mu\text{-}SC_6H_4C_6H_4S\text{-}\mu\text{-}4')$ (**D**), and $[(\mu\text{-S}^-)Fe_2(CO)_6]_2[4\text{-}\mu\text{-}SC_6H_4OCH_2CH_2OC_6H_4S\text{-}\mu\text{-}4']$ (**E**) (generated in situ via reactions of $(\mu\text{-}S_2)Fe_2(CO)_6$ with RMgBr, Et_3BHLi, $4\text{-}LiC_6H_4C_6H_4Li\text{-}4'$, and $4\text{-}LiC_6H_4OCH_2CH_2OC_6H_4Li\text{-}4'$) were found to react with Ph_2PCl to give a series of novel butterfly Fe/S/P cluster complexes. Treatment of monoanions **A** (R = Et, *p*-MeC_6H_4) with 1 equiv of Ph_2PCl in THF from −78 °C to room temperature gave the single-butterfly Fe_2S_2P complexes $(\mu\text{-RS})(\eta^1\text{-}Ph_2PS\text{-}\eta^1)Fe_2(CO)_6$ (**7**, R = Et; **9**, R = *p*-MeC_6H_4) and $(\mu\text{-RS})(\eta^1\text{-}Ph_2PS\text{-}\eta^1)Fe_2(CO)_5(Ph_2PY)$ (**8**, R = Et, Y = Cl; **10**, R = *p*-MeC_6H_4, Y = *p*-MeC_6H_4), whereas dianions **C**, **D**, and **E** reacted with 2 equiv of Ph_2PCl to give single-butterfly $Fe_2S_2P_2$ complex $(\eta^1\text{-}Ph_2PS\text{-}\eta^1)_2Fe_2(CO)_6$ (**11**) and double-butterfly $Fe_4S_4P_2$ complexes $[(\eta^1\text{-}Ph_2PS\text{-}\eta^1)Fe_2(CO)_6]_2(4\text{-}\mu\text{-}SC_6H_4C_6H_4S\text{-}\mu\text{-}4')$ (**12**) and $[(\eta^1\text{-}Ph_2PS\text{-}\eta^1)Fe_2(CO)_6]_2[4\text{-}\mu\text{-}SC_6H_4OCH_2CH_2OC_6H_4S\text{-}\mu\text{-}4']$ (**13**), respectively. More interestingly, the novel μ_4-S-containing double-butterfly Fe_4S_2P complexes $[(\mu\text{-RS})Fe_2(CO)_6](\mu_4\text{-S})[(\mu\text{-}Ph_2P)Fe_2(CO)_6]$ (**14**, R = Me; **15**, R = Ph; **16**, R = Et) could be prepared by reactions of single-butterfly complexes $(\mu\text{-RS})(\eta^1\text{-}Ph_2PS\text{-}\eta^1)Fe_2(CO)_6$ (**1**, R = Me; **3**, R = Ph; **7** R = Et) with excess $Fe_2(CO)_9$ in THF at room temperature, whereas the quadruple-butterfly $Fe_8S_4P_2$ complexes $[(\mu\text{-}Ph_2P)Fe_2(CO)_6(\mu_4\text{-S})Fe_2(CO)_6]_2(4\text{-}\mu\text{-}SC_6H_4C_6H_4S\text{-}\mu\text{-}4')$ (**17**) and $[(\mu\text{-}Ph_2P)Fe_2(CO)_6(\mu_4\text{-S})Fe_2(CO)_6]_2[4\text{-}\mu\text{-}SC_6H_4OCH_2CH_2OC_6H_4S\text{-}\mu\text{-}4']$ (**18**) were similarly prepared by reactions of the corresponding double-butterfly complexes **12** and **13** with excess $Fe_2(CO)_9$, respectively. All the new complexes **7**−**18** have been characterized by elemental analysis, by spectroscopy, and for **9**, **11**, and **14** by X-ray crystallography. In view of the structural similarity of these Fe/S/P complexes to the [FeFe]-hydrogenase active site, they might be regarded as H-cluster models. As a representative, model complex **11** was found to be able to catalyze proton reduction to hydrogen under CV conditions.

Introduction

Although Reihlen prepared the first dinuclear Fe/S cluster complex $(\mu\text{-RS})_2Fe_2(CO)_6$ (R = Et) as early as 1928,[1] the butterfly-shaped Fe_2S_2 structures of such complexes were confirmed only in 1963 by means of X-ray crystal diffraction techniques.[2] In view of their unique structures and the potentially novel reactivities, Seyferth and co-workers began in the 1970s to systematically study the chemistry of such butterfly Fe/S cluster complexes, which was then thought to be nearly mature at the end of the 1990s.[3,4] However, just around this period of time research interest in butterfly Fe/S cluster complexes was extensively revived. This is due to the realization that the active site of [FeFe]-hydrogenases (so-called H-clusters) resembles the archetypal $(\mu\text{-RS})_2Fe_2(CO)_6$ derivatives, which consist of a butterfly Fe_2S_2 cluster core and four unusual ligands: CO, CN^-, $[Fe_4S_4(SCys)_4]$, and a dithiolate (Figure 1).[5] So far, a great variety of butterfly Fe/S cluster complexes that act as structural and functional models of the H-cluster have been prepared and characterized, which has considerably promoted our understanding of the natural enzymes.[6,7] Recently, we published a

---

* To whom correspondence should be addressed. Fax: 0086-22-23504853. E-mail: lcsong@nankai.edu.cn.

(1) Reihlen, H.; von Friedolsheim, A.; Oswald, W. *J. Liebigs Ann. Chem.* **1928**, *465*, 72.

(2) Dahl, L. F.; Wei, C. H. *Inorg. Chem.* **1963**, *2*, 328.

(3) (a) For reviews, see for example: Markó, L.; Markó-Monostory, B. In *The Organic Chemistry of Iron*; von Gustorf, E. A. K., Grevels, F.-W., Fischer, I., Eds.; Academic Press: New York, 1981; pp 283−332. (b) Ogino, H.; Inomata, S.; Tobita, H. *Chem. Rev.* **1998**, *98*, 2093. (c) Song, L.-C. In *Advances in Organometallic Chemistry*; Huang, Y., QianY., Eds.; Chemical Industry Press: Beijing, 1987; pp 181−204. (d) Song, L.-C. *Trends Organomet. Chem.* **1999**, *3*, 1–20.

(4) (a) Seyferth, D.; Henderson, R. S. *J. Am. Chem. Soc.* **1979**, *101*, 508. (b) Nametkin, N. S.; Tyurin, V. D.; Kukina, M. A. *J. Organomet. Chem.* **1978**, *149*, 355. (c) Seyferth, D.; Song, L.-C.; Henderson, R. S. *J. Am. Chem. Soc.* **1981**, *103*, 5103. (d) Seyferth, D.; Henderson, R. S.; Song, L.-C. *Organometallics* **1982**, *1*, 125. (e) Winter, A.; Zsolnai, L.; Huttner, C. *Z. Naturforsch.* **1982**, *37b*, 1430. (f) Bose, K. S.; Sinn, E.; Averill, B. A. *Organometallics* **1984**, *3*, 1126. (g) Seyferth, D.; Ruschke, D. P.; Davis, W. M.; Cowie, M.; Hunter, A. D. *Organometallics* **1994**, *13*, 3834. (h) Song, L.-C.; Yan, C.-G.; Hu, Q.-M.; Wu, B.-M.; Mak, T. C. W. *Organometallics* **1997**, *16*, 632. (i) Seyferth, D.; Kiwan, A. M.; Sinn., E. *J. Organomet. Chem.* **1985**, *281*, 111. (j) Song, L.-C.; Lu, G.-L.; Hu, Q.-M.; Fan, H.-T.; Chen, Y.; Sun, J. *Organometallics* **1999**, *18*, 3258. (k) Song, L.-C.; Lu, G.-L.; Hu, Q.-M.; Sun, J. *Organometallics* **1999**, *18*, 5429.

(5) (a) Peters, J. W.; Lanzilotta, W. N.; Lemon, B. J.; Seefeldt, L. C *Science* **1998**, *282*, 1853. (b) Nicolet, Y.; Piras, C.; Legrand, P.; Hatchikian, C. E.; Fontecilla-Camps, J. C. *Structure* **1999**, *7*, 13.

(6) (a) For reviews, see for example: Darensbourg, M. Y.; Lyon, E. J.; Smee, J. J. *Coord. Chem. Rev.* **2000**, *206−207*, 533. (b) Evans, D. J.; Pickett, C. J. *Chem. Soc. Rev.* **2003**, *32*, 268. (c) Song, L.-C. *Acc. Chem. Res.* **2005**, *38*, 21. (d) Vignais, P. M.; Billoud, B. *Chem. Rev.* **2007**, *107*, 4206. (e) Fontecilla-Camps, J. C.; Volbeda, A.; Cavazza, C.; Nicolet, Y. *Chem. Rev.* **2007**, *107*, 4273. (f) Siegbahn, P. E. M.; Tye, J. W.; Hall, M. B. *Chem. Rev.* **2007**, *107*, 4414.

10.1021/om800077c CCC: $40.75

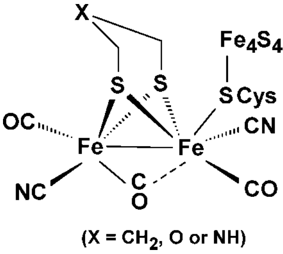

Figure 1. Basic structure of the H-cluster obtained from protein crystallography.

communication[8] that describes the unexpected formation of the Fe/S/P cluster complexes **1**−**6** from reactions of the butterfly Fe/S cluster anions **A** (R = Me, Ph) and **B** (R = *n*-Bu, Ph) with Ph_2PCl (Scheme 1). Since these Fe/S/P complexes contain a butterfly Fe_2S_2 or Fe_2S_2P cluster core that carries a given amount of CO ligands, they might be regarded as the structural analogues of the active site of [FeFe]-hydrogenases.[5] In order to show the generality of such new reactions that produce the interesting Fe/S/P complexes, we further carried out the reactions of Ph_2PCl with other butterfly Fe/S cluster anions, such as (μ-RS)(μ-S^-)$Fe_2(CO)_6$ (**A**, R = Et, *p*-MeC_6H_4), (μ-S^-)$_2Fe_2(CO)_6$ (**C**), [(μ-S^-)$Fe_2(CO)_6$]$_2$(4-μ-$SC_6H_4C_6H_4S$-μ-4′) (**D**), and [(μ-S^-)$Fe_2(CO)_6$]$_2$[4-μ-$SC_6H_4OCH_2CH_2OC_6H_4S$-μ-4′] (**E**). As a result, the reactions afforded a series of expected single- and double-butterfly Fe/S/P cluster complexes. Particularly, when such single- and double-butterfly complexes were further treated with $Fe_2(CO)_9$, another series of novel μ_4-S-containing double- and quadruple-butterfly Fe/S/P complexes were unexpectedly produced. In addition, the single-butterfly Fe/S/P complex (η^1-Ph_2PS-η^1)$_2Fe_2(CO)_6$ has been found to be a catalyst for proton reduction to H_2 under electrochemical conditions. Herein we report these interesting results.

Results and Discussion

Synthesis and Characterization of Single-Butterfly Fe_2S_2P/$Fe_2S_2P_2$ Complexes 7−11 and Double-Butterfly $Fe_4S_4P_2$ Complexes 12 and 13. As mentioned above, the single- and double-butterfly complexes **1**−**6** can be prepared by reactions of the BrMg salts of monoanions **A** (R = Me, Ph) and the lithium salts of monoanions **B** (R = *n*-Bu, Ph) with Ph_2PCl, respectively (Scheme 1).[8] Similarly, we could further prepare the single-butterfly Fe_2S_2P complexes **7**−**10** by treatment of the BrMg salts of monoanions **A** (R = Et, *p*-MeC_6H_4) (prepared in situ from 1 equiv of (μ-S_2)$Fe_2(CO)_6$ and 1 equiv of the Grignard reagents RMgBr)[9] with 1 equiv of Ph_2PCl in THF from −78 °C to room temperature (Scheme 2).

Although the mechanism for formation of **7**−**10** is not clear to date, the previously suggested mechanism for formation of **1**−**4**[8] should apply to the formation of **7**−**10** since both cases involve the same type of highly nucleophilic S-centered monoanions **A** and give the same type of products. As shown in Scheme 2, the nucleophilic substitution between monoanions **A** and Ph_2PCl will first give the butterfly Fe/S cluster phosphines $\mathbf{M_1}$. Then, major products **7** and **9** can be produced from $\mathbf{M_1}$ by nucleophilic attack of its P atom at the neighboring iron atom accompanied by displacement of mercaptide from it.[10] The minor products **8** and **10** can be produced by further CO substitution of **7** or **9** with unreacted Ph_2PCl or $Ph_2PC_6H_4Me$-*p* (formed in situ from Ph_2PCl and the Grignard reagent *p*-MeC_6H_4MgBr present in the reaction system), respectively.

The single-butterfly $Fe_2S_2P_2$ complex **11** and double-butterfly $Fe_4S_4P_2$ complexes **12** and **13** could also be prepared from Ph_2PCl and the corresponding dianions **C**, **D**, and **E**, respectively. Treatment of 1 equiv of the dilithium salt of dianion **C** (generated in situ from (μ-S_2)$Fe_2(CO)_6$ and 2 equiv of Et_3BHLi)[11] with 2 equiv of Ph_2PCl in THF from −78 °C to room temperature afforded the single-butterfly complex **11** (Scheme 3), whereas treatment of 2 equiv of Ph_2PCl with ca. 1 equiv of the dilithium salt of dianion **D** (formed by reaction of 1 equiv of 4,4′-dibromodiphenyl with 2 equiv of *n*-BuLi followed by treatment of the intermediate 4-$LiC_6H_4C_6H_4Li$-4′[12] with (μ-S_2)$Fe_2(CO)_6$)[13] or treatment of 2 equiv of Ph_2PCl with ca. 1 equiv of the dilithium salts of dianions **E** (generated similarly by reaction of 1 equiv of the ether chain-bridged 4,4′-dibromodiphenyls with 2 equiv of *n*-BuLi followed by treatment of the intermediate 4-$LiC_6H_4OCH_2CH_2OC_6H_4Li$-4′[12] with ($\mu$-$S_2$)$Fe_2(CO)_6$)[13] gave rise to the double-butterfly complexes **12** (Scheme 4) and **13** (Scheme 5), respectively.

Complexes **7**−**13** are air-stable solids, which have been characterized by elemental analysis and IR, ^{1}H NMR, and ^{31}P NMR spectroscopies. For example, the IR spectra of **8** and **10** displayed four absorption bands in the range 2040−1934 cm^{-1} for their terminal carbonyls, whereas those of **7**, **9**, and **11**−**13** exhibited four to six absorption bands in the region 2070−1958 cm^{-1} for their terminal carbonyls. Compared to the highest $\nu_{C\equiv O}$ frequencies of **7**, **9**, and **11**−**13**, those of **8** and **10** are shifted by ca. 30 cm^{-1} toward lower values due to the stronger electron-donating effects of $Ph_2P(C_6H_4Me$-*p*) and Ph_2PCl than CO.[14] In addition, the ^{31}P NMR spectra of **8** and **10** each showed two singlets at ca. 71 and 151 and ca. 58 and 70 ppm, respectively, for P atoms in their Ph_2PS, Ph_2PCl, and $Ph_2P(C_6H_4Me$-*p*) ligands, whereas those of **7**, **9**, and **11**−**13** all displayed one singlet in the range 44−67 ppm for P atoms in their Ph_2PS ligands.

In order to unequivocally confirm the butterfly Fe_2S_2P cluster cores present in complexes **7**−**10**, **12**, and **13**, as well as the butterfly $Fe_2S_2P_2$ cluster core present in complex **11**, we determined the crystal structures of complexes **9** and **11** by X-ray diffraction techniques. ORTEP plots of **9** and **11** are presented in Figures 2 and 3, whereas Table 1 shows selected bond lengths and angles. As can be seen in Figure 2, complex **9** is actually isostructural with the previously reported complex **1**,[8] which contains a butterfly Fe(1)Fe(2)S(1)P(1)S(2) cluster

---

(7) (a) Gloaguen, F.; Lawrence, J. D.; Schmidt, M.; Wilson, S. R.; Rauchfuss, T. B. *J. Am. Chem. Soc.* **2001**, *123*, 12518. (b) Lyon, E. J.; Georgakaki, I. P.; Reibenspies, J. H.; Darensbourg, M. Y. *J. Am. Chem. Soc.* **2001**, *123*, 3268. (c) Razavet, M.; Davies, S. C.; Hughes, D. L.; Barclay, J. E.; Evans, D. J.; Fairhurst, S. A.; Liu, X.; Pickett, C. J. *Dalton Trans.* **2003**, 586. (d) Lawrence, J. D.; Li, H.; Rauchfuss, T. B. *Chem. Commun.* **2001**, 1482. (e) Song, L.-C.; Ge, J.-H.; Zhang, X.-G.; Liu, Y.; Hu, Q.-M. *Eur. J. Inorg. Chem.* **2006**, 3204. (f) Song, L.-C.; Yang, Z.-Y.; Hua, Y.-J.; Wang, H.-T.; Liu, Y.; Hu, Q.-M. *Organometallics* **2007**, *26*, 2106. (g) Morvan, D.; Capon, J.-F.; Gloaguen, F.; Le Goff, A.; Marchivie, M.; Michaud, F.; Schollhammer, P.; Talarmin, J.; Yaouanc, J.-J. *Organometallics* **2007**, *26*, 2042.

(8) Song, L.-C.; Zeng, G.-H.; Hu, Q.-M.; Ge, J.-H.; Lou, S.-X. *Organometallics* **2005**, *24*, 16.

(9) Seyferth, D.; Henderson, R. S.; Song, L.-C.; Womack, G. B. *J. Organomet. Chem.* **1985**, *292*, C9.

(10) Seyferth, D.; Womack, G. B.; Song, L.-C.; Cowie, M.; Hames, B. W. *Organometallics* **1983**, *2*, 928.

(11) Seyferth, D.; Henderson, R. S.; Song, L.-C. *J. Organomet. Chem.* **1980**, *192*, C1.

(12) Baldwin, R. A.; Cheng, M. T. *J. Org. Chem.* **1967**, *32*, 1572.

(13) (a) Seyferth, D.; Song, L.-C.; Henderson, R. S. *J. Am. Chem. Soc.* **1981**, *103*, 5103. (b) Seyferth, D.; Henderson, R. S. *J. Am. Chem. Soc.* **1979**, *101*, 508.

(14) Collman, J. P.; Hegedus, L. S.; Norton, J. R.; Finke, R. G. *Principles and Applications of Organotransition Metal Chemistry*, 2nd ed.; California University Science Books: Mill Valley, 1987.

Scheme 1

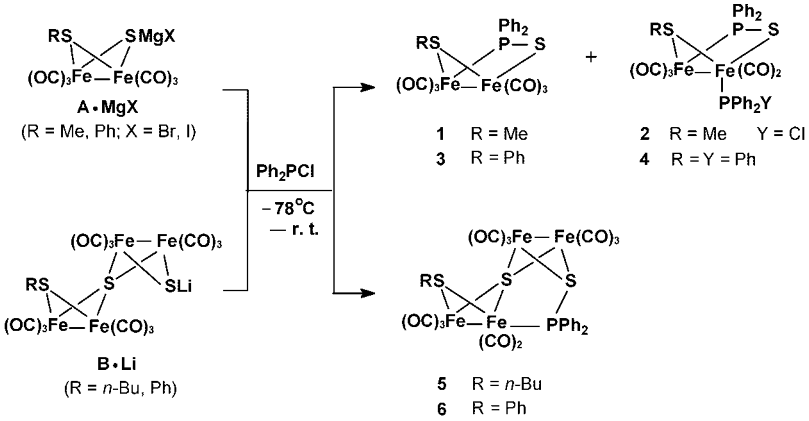

Scheme 2

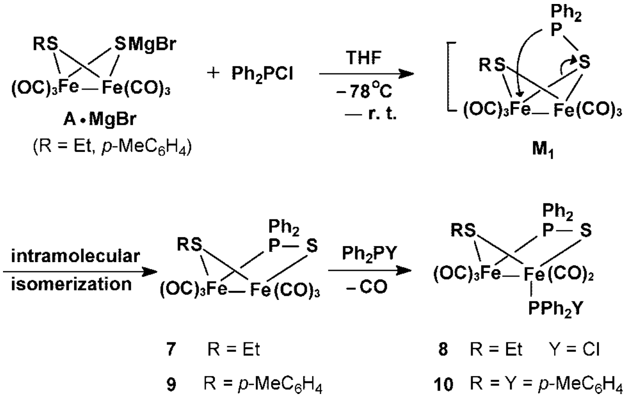

Scheme 3

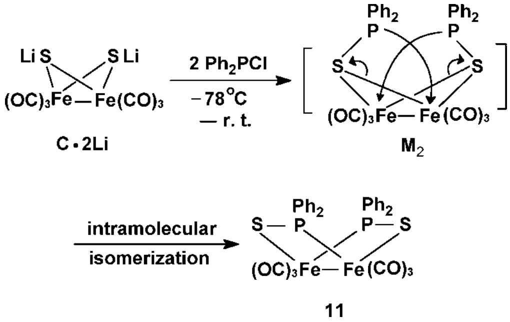

core that carries two phenyl groups, one p-MeC$_6$H$_4$ group, and six terminal carbonyls. The X-ray crystallographic study revealed that the dihedral angle of **9** between its triangular wing Fe(1)Fe(2)S(2) and tetragonal wing Fe(1)Fe(2)P(1)S(1) is 90.3°, which is almost the same as the corresponding one of **1** (89.1°). In addition, the S(2) atom of **9** is attached to the substituent p-MeC$_6$H$_4$ group by an equatorial bond in order to avoid the strong steric repulsion with one of the two phenyl groups attached to P(1).[15] The X-ray crystallographic study of complex **11** (Figure 3) indicated that it consists of a butterfly Fe(1)Fe(2)-P(1)S(1)P(2)S(2) cluster core in which the P(1)/P(2) atoms each carry two phenyl groups and the Fe(1)/Fe(2) atoms are each attached to three terminal carbonyls. The dihedral angle of **11** between its two tetragonal wings Fe(1)Fe(2)P(1)S(1) and Fe(1)Fe(2)P(2)S(2) is 87.4°. The Fe−Fe bond length of **11** (2.7790 Å) is much longer than the corresponding bond lengths of **1** (2.6431 Å)[8] and particularly (μ-EtS)$_2$Fe$_2$(CO)$_6$ (2.537 Å).[2]

Scheme 4

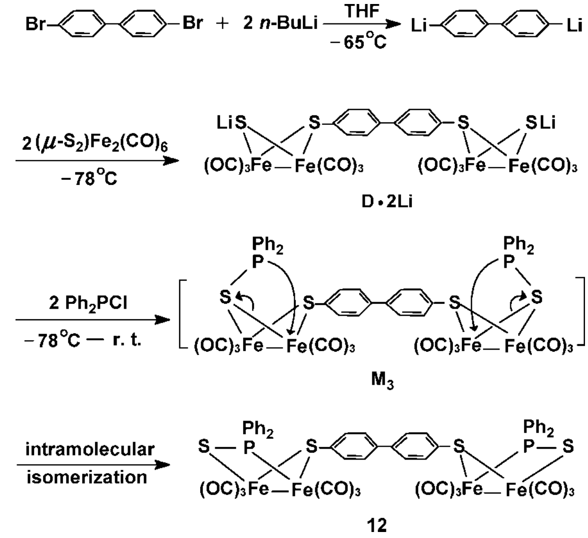

Scheme 5

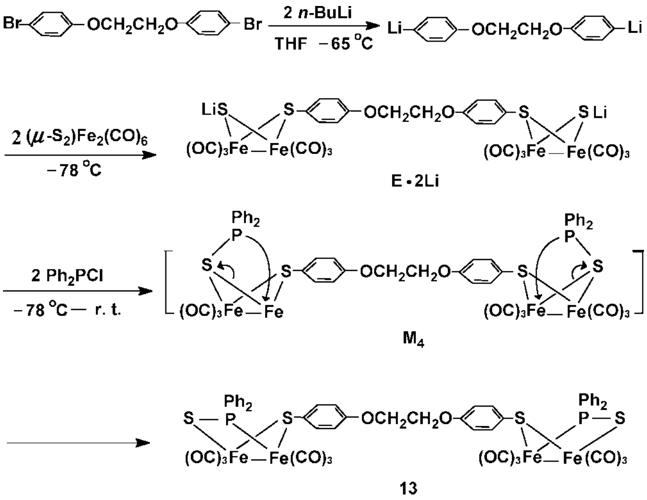

This is obviously because the Fe−Fe bond of **11** is bridged by two diatom (P, S) units, that of **1** by one diatom (P, S) unit and one monoatom (S) unit and that of (μ-EtS)$_2$Fe$_2$(CO)$_6$ by two monoatom (S, S) units. It is worth pointing out that **11** is the first butterfly Fe/S/P complex with two tetragonal wings, although some butterfly Fe/S/P complexes are known to have one triangular wing and one tetragonal wing, such as the previously reported **1**−**4**, or to have two triangular wings such

---

[15] Shaver, A.; Fitzpatrick, P. J.; Steliou, K.; Butler, I. S. *J. Am. Chem. Soc.* **1979**, *101*, 1313.

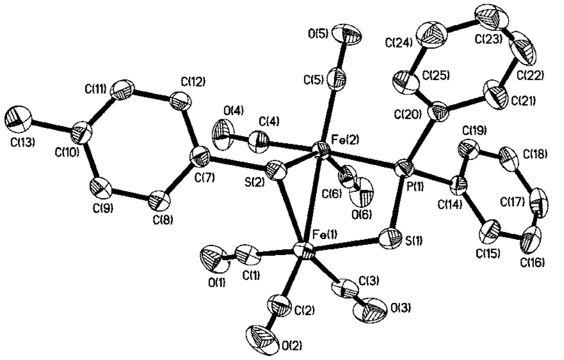

Figure 2. Molecular structure of **9** with 30% probability level ellipsoids.

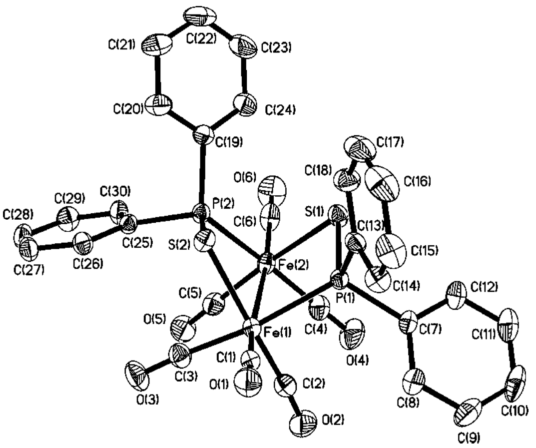

Figure 3. Molecular structure of **11** with 30% probability level ellipsoids.

as (μ-Ph_2P)(μ-RS)$Fe_2(CO)_6$ (R = Ph,[16] Et,[17] C_6H_{11}[18]), (μ-PhPCl)(μ-*t*-BuS)$Fe_2(CO)_6$,[19] and (μ-Me_2P)(μ-*t*-BuS)$Fe_2(CO)_6$.[20]

Synthesis and Characterization of Double-Butterfly Fe_4S_2P Complexes 14−16 and Quadruple-Butterfly $Fe_8S_4P_2$ Complexes 17 and 18. In order to examine the chemical reactivities of the above-prepared Fe/S/P cluster complexes, we chose some of the prepared complexes such as **1**, **3**, **7**, **12**, and **13** to react with $Fe_2(CO)_9$ to see if the higher nuclearity Fe/S/P cluster complexes could be obtained. The higher nuclearity double-butterfly Fe_4S_2P complexes **14**−**16** were prepared upon treatment of single-butterfly Fe_2S_2P complexes **1**, **3**, and **7** with excess $Fe_2(CO)_9$ in THF at room temperature (Scheme 6), whereas the higher nuclearity quadruple-butterfly $Fe_8S_4P_2$ complexes **17** and **18** could be obtained by reactions of double-butterfly $Fe_4S_4P_2$ complexes **12** and **13** with excess $Fe_2(CO)_9$ under similar conditions (Scheme 7).

Scheme 6

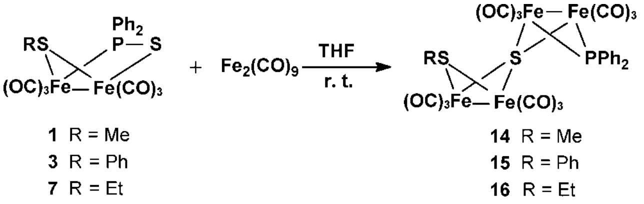

Table 1. Selected Bond Lengths (Å) and Angles (deg) for 9, 11, and 14

		9	
Fe(1)−S(2)	2.2424(14)	Fe(2)−S(2)	2.2767(13)
Fe (1)-S(1)	2.3655(14)	P(1)−S(1)	2.0336(15)
Fe(2)−P(1)	2.2772(13)	S(2)−C(7)	1.789 (4)
P(1)−C(14)	1.824(4)	Fe(1)−Fe(2)	2.6327(9)
S(2)−Fe(1)−S(1)	83.22(4)	P(1)−Fe(2)−Fe(1)	77.35(4)
S(2)−Fe(1)−Fe(2)	54.98(3)	S(1)−P(1)−Fe(2)	104.77(6)
S(1)−Fe(1)−Fe(2)	86.12(4)	Fe(1)−S(2)−Fe(2)	71.26(4)
S(2)−Fe(2)−P(1)	87.47(5)	S(2)−Fe(2)−Fe(1)	53.77(4)
		11	
Fe(1)−P(1)	2.2576(16)	P(1)−C(7)	1.830(5)
Fe(1)−S(2)	2.3487(17)	P(1)−S(1)	2.027(2)
Fe(2)−P(2)	2.2602(16)	S(2)−P(2)	2.032(2)
Fe(2)−S(1)	2.3469(17)	Fe(1)−Fe(2)	2.7790(13)
S(2)−Fe(1)−P(1)	86.12(6)	S(2)−Fe(1)−Fe(2)	83.78(5)
S(2)−P(2)−Fe(2)	106.36(8)	S(1)−Fe(2)−Fe(1)	83.50(5)
P(1)−S(1)−Fe(2)	90.55(7)	P(2)−Fe(2)−S(1)	87.20(6)
P(2)−S(2)−Fe(1)	89.76(7)	P(2)−Fe(2)−Fe(1)	75.13(5)
		14	
Fe(1)−P(1)	2.223(2)	Fe(3)−Fe(4)	2.5118(17)
Fe(1)−S(1)	2.263(2)	Fe(1)−Fe(2)	2.5889(17)
Fe(2)−P(1)	2.223(2)	Fe(3)−S(1)	2.260(2)
Fe(2)−S(1)	2.229(2)	Fe(4)−S(1)	2.275(2)
P(1)−Fe(1)−S(1)	80.79(8)	Fe(1)−P(1)−Fe(2)	71.22(8)
S(1)−Fe(1)−Fe(2)	54.20(6)	Fe(2)−S(1)−Fe(3)	139.25(10)
P(1)−Fe(2)−Fe(1)	54.40(7)	Fe(3)−S(1)−Fe(4)	67.27(7)
S(1)−Fe(2)−Fe(1)	55.42(6)	Fe(4)−S(2)−Fe(3)	67.49(7)

It is apparent that the formation of **14**−**18** is actually the consequence of the transformation of each Ph_2-substituted tetragonal Fe_2SP wing in the starting butterfly Fe/S/P complexes to the (μ-Ph_2P)$Fe_2(CO)_6$-substituted Fe_2S triangular wing. Although the mechanism regarding this type of transformation is not completely understood, a possible transformation pathway (Scheme 8) might be proposed according to the following facts: (i) $Fe_2(CO)_9$ in THF solution at room temperature is known to give the intermediate $Fe(CO)_4$(THF), from which the heteroatom nitrogen donors can displace the THF,[21] and (ii) the coordination unsaturated species, such as $Cr(CO)_5$, can readily add to a metal-attached S atom to give the nuclearity increased metal cluster.[22] The pathway includes the following steps: (i) the heteroatom S in the tetragonal Fe_2SP wing of the single-butterfly Fe_2S_2P cluster $\mathbf{m_1}$ attacks the Fe atom of one molecule of $Fe(CO)_4$(THF) (generated in situ from $Fe_2(CO)_9$ and THF) to give intermediate $\mathbf{m_2}$; (ii) further intramolecular attack of the same S atom at its neighboring Fe atom with displacement of Ph_2P from it affords intermediate $\mathbf{m_3}$ (the favored isomerization from tetragonal Fe_2SP wing to triangular Fe_2S wing is presumably due to coordination of the S atom with $Fe(CO)_4$); (iii) the pendant Ph_2P group of $\mathbf{m_3}$ displaces THF of another molecule of $Fe(CO)_4$(THF) to produce intermediate $\mathbf{m_4}$; and finally (iv) the double-butterfly Fe_4S_2P cluster $\mathbf{m_5}$ is formed by steps such as loss of two CO ligands from the two $Fe(CO)_4$ units and formation of the new Fe−Fe, Fe−S, and Fe−P bonds followed by cleavage of the old P−S bond. It should be noted that this butterfly cluster transformation mechanism for formation of

---

(16) Job, B. E.; Mclean, R. A. N.; Thompson, D. T. *J. Chem. Soc., Chem. Commun.* **1966**, 895.

(17) Seyferth, D.; Womack, G. B.; Dewan, J. C. *Organometallics* **1985**, *4*, 398.

(18) Winter, A.; Zsolnai, L.; Huttner, G. *J. Organomet. Chem.* **1983**, *250*, 409.

(19) Song, L.-C.; Wang, R.-J.; Li, Y.; Wang, H.-G.; Wang, J.-T. *Chin. J. Org. Chem* **1989**, *9*, 512.

(20) Song, L.-C.; Hu, Q.-M.; Zhou, Z.-Y.; Hu, G.-Z. *Chin. J. Org. Chem* **1991**, *11*, 533.

(21) Cotton, F. A.; Troup, J. M. *J. Am. Chem. Soc.* **1974**, *96*, 3438.

(22) Richter, F.; Vahrenkamp, H. *Angew. Chem., Int. Ed. Engl.* **1978**, *17*, 444.

Scheme 7

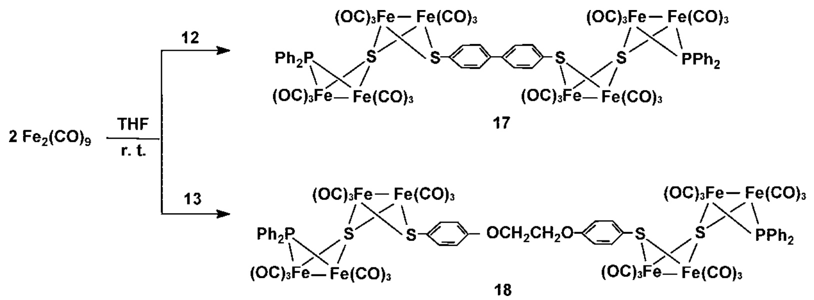

Scheme 8

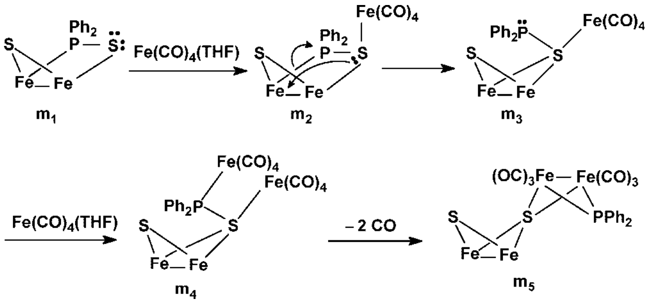

14−**18** seems to be reasonable, but it is mainly speculative. So, more work needs to be done in the future.

Complexes **14**−**18** are also air-stable solids, which were characterized by elemental analysis and various spectroscopies. For example, the IR spectra of **14**−**18** showed four to six absorption bands in the region 2079−1943 cm^{-1} for their terminal carbonyls. The ^{1}H NMR spectra of **14** and **16** each displayed a singlet at 2.07 and 1.33 ppm for CH$_3$ protons in their MeS and EtS groups, whereas the spectrum of **18** exhibited an AB quartet in the range 6.7−7.2 ppm for its two phenylene groups. In addition, the ^{31}P NMR spectra of **14**−**18** displayed a singlet at ca. 145 ppm for P atoms in their Ph$_2$P groups, very close to those displayed by P atoms in complexes (μ-Ph$_2$P)(μ-RS)Fe$_2$(CO)$_6$ (R = C$_6$H$_{11}$,[18] R = *n*-Pr, *i*-Pr, *t*-Bu[23]) and [(μ-Ph$_2$P)Fe$_2$(CO)$_6$]$_2$[μ-SCH$_2$(CH$_2$OCH$_2$)$_2$CH$_2$S-μ].[24]

To further confirm the μ_4-S-containing double-butterfly Fe$_4$S$_2$P cluster cores present in complexes **14**−**18**, X-ray diffraction analysis for the representative complex **14** was undertaken. The molecular structure of **14** is depicted in Figure 4, whereas selected bond lengths and angles are listed in Table 1. Complex **14** is composed of two butterfly subclusters, Fe(1)Fe(2)S(1)P(1) and Fe(3)Fe(4)S(1)S(2), joined to a pyran type of μ_4-S(1) atom. While the S(2) atom is attached to C(13) of the methyl group by an equatorial bond, the P(1) atom is attached to C(14) and C(20) of the two phenyl groups by an equatorial and an axial bond,[13] respectively. In addition, each of the three carbonyls attached to Fe(1), Fe(2), Fe(3), and Fe(4) are terminal. In butterfly subcluster Fe(1)Fe(2)S(1)P(1) the dihedral angle between its two triangular wings is 105.9°, which is obviously larger than the corresponding dihedral angle (96.81°) in subcluster Fe(3)Fe(4)S(1)S(2). In addition, the Fe(1)−Fe(2) bond length (2.5889 Å) is slightly longer than the Fe(3)−Fe(4) bond length (2.5118 Å). It should be noted that complexes **14**−**18** are the first butterfly Fe/S/P complexes with two different subclusters, Fe$_2$S$_2$ and Fe$_2$SP, joined together through a common μ_4-S atom, although numerous μ_4-E (E = S, Se)-containing butterfly cluster complexes are known, such as [(μ-RS)Fe$_2$(CO)$_6$]$_2$(μ_4-S) (R=Me,[25] Et[26]), [(μ-EtS)Fe$_2$(CO)$_6$][(μ-PhC≡CS)Fe$_2$(CO)$_6$](μ_4-S),[27] [(μ-EtS)Fe$_2$(CO)$_6$]$_2$(μ_4-Se),[28] and [(μ-EtTe)Fe$_2$(CO)$_6$]$_2$(μ_4-S).[29]

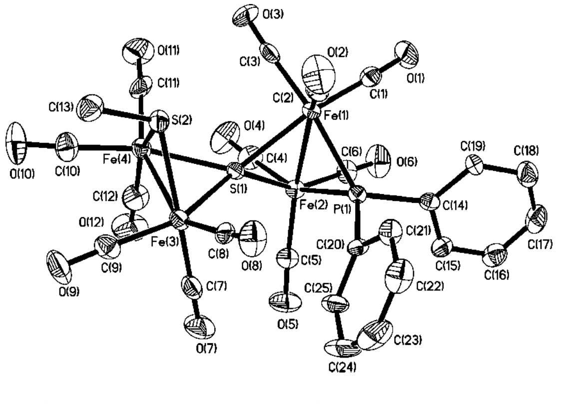

Figure 4. Molecular structure of **14** with 30% probability level ellipsoids.

Electrochemistry of Complex 11. The electrochemical properties of **11** were studied by cyclic voltammetry (CV) in MeCN solution under an atmosphere of N$_2$. As shown in Figure 5, the cyclic voltammogram of **11** shows two irreversible one-electron reductions at E_{pc}= −1.32 and − 2.09 V and one irreversible one-electron oxidation at E_{pa} = + 0.74 V, which could be ascribed to the Fe^{I}Fe^I/Fe^{I}Fe^0, Fe^{I}Fe^0/Fe^{0}Fe^0, and Fe^{I}Fe^I/Fe^{I}Fe^{II} couples, respectively. The one-electron assignments for these redox processes were supported by the calculated value of 0.95 faraday/equiv (obtained through study of bulk electrolysis of a MeCN solution of **11**) and the calculated value of $(i_p/\nu^{1/2})/(it^{1/2})$ = 3.3 (obtained through study of CV and chronoamperometry (CA) of **11**).[30] The cyclic voltammograms of **11** with HOAc and without HOAc (for comparative purposes) are presented in Figure 6. Interestingly, as shown in Figure 6, when the first 2 mM HOAc was added to the MeCN solution of **11**, the original first reduction peak at −1.32 V did not change, but the second reduction peak at − 2.09 V considerably increased and continued to grow up with sequential addition of the acid. Apparently, these observations are characteristic of an electrocatalytic proton reduction process.[31–33] More interest-

---

(23) Song, L.-C.; Li, Y.; Hu, Q.-M.; Wang, J.-T.; Zhao, W.-J.; Fan, Y.-Q.; Zhang, S.-J.; Li, X.-Q.; Li, G.-W. *Chem. J. Chin. Univ.* **1990**, *11*, 154.

(24) Song, L.-C.; Fan, H.-T.; Hu, Q.-M.; Yang, Z.-Y.; Sun, Y.; Gong, F.-H. *Chem.−Eur. J.* **2003**, *9*, 170.

(25) Coleman, J. M.; Wojcicki, A.; Pollick, P. J.; Dahl, L. F. *Inorg. Chem.* **1967**, *6*, 1236.

(26) Seyferth, D.; Kiwan, A. M. *J. Organomet. Chem.* **1985**, *286*, 219.

(27) Song, L.-C.; Qin, X.-D.; Hu, Q.-M.; Huang, X.-Y. *Organometallics* **1998**, *17*, 5437.

(28) Song, L.-C.; Yan, C.-G.; Hu, Q.-M.; Wang, R.-J.; Mak, T. C. W.; Huang, X.-Y. *Organometallics* **1996**, *15*, 1535.

(29) Song, L.-C.; Hu, Q.-M.; Sun, B.-W.; Tang, M.-Y.; Yang, J; Hua, Y.-J. *Organometallics* **2002**, *21*, 1627.

(30) Zanello, P. *Inorganic Electrochemistry. Theory, Practice and Application*; Thomas Graham House: Cambridge, UK, 2003.

(31) Bhugun, I.; Lexa, D.; Saveant, J.-M. *J. Am. Chem. Soc.* **1996**, *118*, 3982.

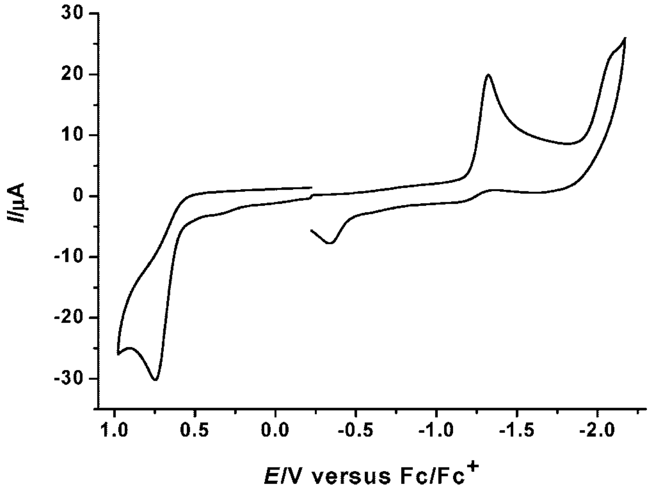

Figure 5. Cyclic voltammogram of **11** (1.0 mM) in 0.1 M *n*-Bu$_4$NPF$_6$/MeCN at a scan rate of 100 mV s^{-1}.

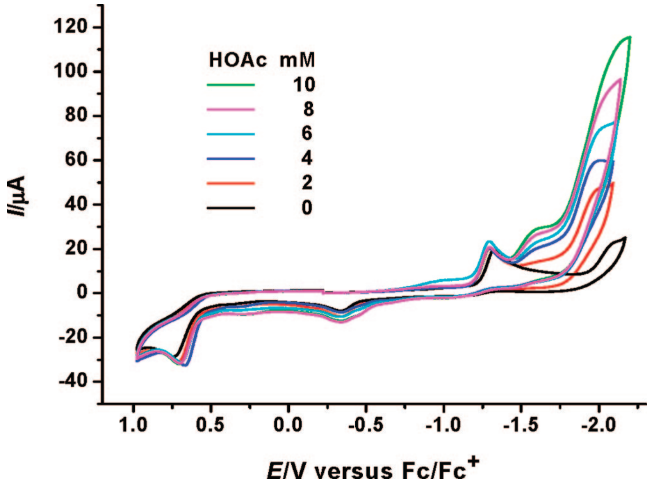

Figure 6. Cyclic voltammogram of **11** (1.0 mM) with HOAc (0−10 mM) in 0.1 M *n*-Bu$_4$NPF$_6$/MeCN at a scan rate of 100 mV s^{-1}.

ingly, this process was further proved by bulk electrolysis of a MeCN solution of **11** (0.5 mM) with HOAc (25 mM) at −2.20 V. During 0.5 h of the bulk electrolysis, 10.2 F per mol of **11** was passed, which corresponds to 5.1 turnovers. H$_2$ bubbles could be seen during the large-scale electrolytic experiment. GC analysis showed that the hydrogen yield was nearly 100%.

Conclusion

We have synthesized and characterized a series of new butterfly Fe/S/P cluster complexes, which include (i) complexes **7**−**10**, having one butterfly Fe$_2$S$_2$P cluster core, (ii) complex **11**, having one butterfly Fe$_2$S$_2$P$_2$ cluster core, (iii) complexes **12** and **13**, having two butterfly Fe$_2$S$_2$P cluster cores, (iv) complexes **14**−**16**, containing one double-butterfly Fe$_4$S$_2$P core with a common μ_4-S atom, and (v) complexes **17** and **18**, containing two double-butterfly Fe$_4$S$_2$P cluster cores each with a common μ_4-S atom. Interestingly, while **7**−**13** were synthesized via a novel type of reactions of the S-centered butterfly anions **A** (R = Et, *p*-MeC$_6$H$_4$), **C**, **D**, and **E** with Ph$_2$PCl, complexes **14**−**18** could be prepared by another novel type of reactions of complexes **1**, **3**, **7**, **12**, and **13** with Fe$_2$(CO)$_9$, respectively. That is, the first type of reactions can accomplish the conversion from the S-centered triangular Fe$_2$S wings in anions **A**, **C**, **D**, and **E** to the tetragonal Fe$_2$SP wings in complexes **7**−**13**, whereas the second type of reactions can achieve the conversion from the Ph$_2$-substituted tetragonal Fe$_2$SP wings in complexes **1**, **3**, **7**, **12**, and **13** to the (μ-Ph$_2$P)Fe$_2$(CO)$_6$-substituted Fe$_2$S triangular wings in complexes **14**−**18**, respectively. Considering the structural similarity of complexes **7**−**18** to the active site of [FeFe]-hydrogenases, as well as the H$_2$ production catalyzed by complex **11**, these butterfly Fe/S/P complexes might be regarded as H-cluster models. Further studies regarding the formation mechanism for such butterfly Fe/S/P complexes and the electrocatalytic mechanism for proton reduction catalyzed by such complexes are underway.

Experimental Section

General Comments. All reactions were carried out under an atmosphere of prepurified nitrogen using standard Schlenk and vacuum-line techniques. Tetrahydrofuran (THF) was purified by distillation under nitrogen from Na/benzophenone ketyl. (μ-S$_2$)Fe$_2$(CO)$_6$,[34] Fe$_2$(CO)$_9$,[35] RMgBr (R = Et, *p*-MeC$_6$H$_4$),[36] Ph$_2$PCl,[37] 4-BrC$_6$H$_4$C$_6$H$_4$Br-4′,[38] 4-BrC$_6$H$_4$OCH$_2$CH$_2$OC$_6$H$_4$Br-4′,[39] and (μ-RS)(η^1-Ph$_2$PS-η^1)Fe$_2$(CO)$_6$ (R = Me, Ph)[8] were prepared according to the published procedures. *n*-BuLi (1 M in hexane) and Et$_3$BHLi (1 M in THF) were available commercially. While products were separated by preparative TLC (25 × 15 × 0.25 cm) on glass plates coated with silica gel 60 H, samples for analysis were further purified by recrystallization from common organic solvents. IR spectra were recorded on a Nicolet Magna 500 FTIR or a Bruker Vector 22 infrared spectrophotometer. ^{1}H NMR and ^{31}P NMR spectra were taken on a Bruker AC-P200 NMR spectrometer. C/H analyses were performed with an Elementar Vario EL analyzer. Melting points were determined on a Yanaco MP-500 apparatus and are uncorrected.

Preparation of (μ-EtS)(η^1-Ph$_2$PS-η^1)Fe$_2$(CO)$_6$ (7) and (μ-EtS)(η^1-Ph$_2$PS-η^1)Fe$_2$(CO)$_5$(Ph$_2$PCl) (8). A red solution of (μ-S$_2$)Fe$_2$(CO)$_6$ (0.344 g, 1.0 mmol) in THF (20 mL) was cooled to −78 °C under stirring by a dry ice/acetone bath. To this solution was added a diethyl ether solution of EtMgBr (ca. 1 mmol) by syringe until the mixture turned emerald green. The green mixture was stirred at this temperature for 15 min, and then Ph$_2$PCl (0.2 mL, 1.0 mmol) was added to cause an immediate color change to red. The new mixture was allowed to warm to room temperature and stirred at this temperature for 1 h. Volatiles were removed under reduced pressure, and the residue was subjected to TLC separation using CH$_2$Cl$_2$/petroleum ether (1:4 v/v) as eluent. From the first, orange-red band **7** was obtained as a red solid (0.346 g, 62%). Mp: 120−121 °C. Anal. Calcd for C$_{20}$H$_{15}$Fe$_2$O$_6$PS$_2$: C, 43.04; H, 2.71. Found: C, 42.83; H, 2.69. IR (KBr disk): $\nu_{C\equiv O}$ 2066 (vs), 2020 (vs), 2007 (vs), 1992 (vs), 1972 (s), 1958 (s) cm^{-1}. ^{1}H NMR (200 MHz, CDCl$_3$): 1.66 (t, J = 7.2 Hz, 3H, CH$_3$), 2.82 (q, J = 7.2 Hz, 2H, CH$_2$), 7.24−7.78 (m, 10H, 2C$_6$H$_5$) ppm. ^{31}P NMR (81.0 MHz, CDCl$_3$, 85% H$_3$PO$_4$): 66.99 (s) ppm. From the second, brown-red band **8** was obtained as a red solid (0.061 g, 8%). Mp: 151−152 °C. Anal. Calcd for C$_{31}$H$_{25}$ClFe$_2$O$_5$P$_2$S$_2$: C, 49.57; H, 3.33. Found:

---

(32) Chong, D.; Georgakaki, I. P.; Mejia-Rodriguez, R.; Sanabria-Chinchilla, J.; Soriaga, M. P.; Darensbourg, M. Y. *Dalton Trans.* **2003**, *3*, 4158.

(33) Capon, J.-F.; Gloaguen, F.; Schollhammer, P.; Talarmin, J. *Coord. Chem. Rev.* **2005**, *249*, 1664.

(34) Seyferth, D.; Henderson, R. S.; Song, L.-C. *Organometallics* **1982**, *1*, 125.

(35) King, R. B. *Organometallic Syntheses, Transition-Metal Compounds*; Academic Press: New York, 1965; Vol. I, p 95.

(36) Gilman, H.; Zoellner, E. A.; Dickey, J. B. *J. Am. Chem. Soc.* **1929**, *51*, 1576.

(37) Horner, L. *Chem. Ber.* **1961**, *94*, 21.

(38) Buckles, R. E.; Wheeler, N. G. *Org. Synth.* **1951**, *31*, 29.

(39) Tashiro, M.; Sumida, T.; Fukata, G. *J. Org. Chem.* **1980**, *45*, 1156.

Table 2. Crystal Data and Structure Refinement Details for 9, 11, and 14

	9	11	14
mol formula	$C_{25}H_{17}Fe_2O_6PS_2$	$C_{30}H_{20}Fe_2O_6P_2S_2$	$C_{25}H_{13}Fe_4O_{12}PS_2$
mol wt	620.18	714.22	823.84
cryst syst	monoclinic	triclinic	monoclinic
space group	*P*2(1)/*c*	$P\bar{1}$	*Cc*
a/Å	15.333(5)	9.991(4)	10.268(4)
b/Å	10.876(3)	11.558(5)	15.146(7)
c/Å	17.090(5)	14.893(6)	20.165(9)
α/deg	90	71.732(7)	90
β/deg	112.554(5)	88.952(7)	98.215(7)
γ/deg	90	70.292(7)	90
V/Å^3	2632.2(13)	1530.1(11)	3104(2)
Z	4	2	4
D_c/g cm^{-3}	1.565	1.550	1.736
abs coeff/mm^{-1}	1.360	1.231	2.077
F(000)	1256	724	1640
index ranges	$-19 \le h \le 15$	$-12 \le h \le 12$	$-11 \le h \le 12$
	$-13 \le k \le 11$	$-5 \le k \le 13$	$-9 \le k \le 18$
	$-9 \le l \le 21$	$-17 \le l \le 17$	$-23 \le l \le 23$
no. of rflns	12 136	6543	5417
no. of indep rflns	5374	5530	4895
$2\theta_{max}$/deg	52.82	50.70	50.04
R	0.0552	0.0494	0.0490
R_w	0.0734	0.0945	0.0710
goodness of fit	0.961	0.992	1.043
largest diff peak and hole/e Å^{-3}	0.411/−0.377	0.469/−0.464	0.376/−0.349

C, 49.70; H, 3.48. IR (KBr disk): $\nu_{C\equiv O}$ 2039 (vs), 1985 (vs), 1953 (vs), 1941 (s) cm^{-1}. ^{1}H NMR (200 MHz, $CDCl_3$): 1.42 (t, *J* = 7.2 Hz, 3H, CH_3), 2.35−2.50 (m, 2H, CH_2), 7.27−7.97 (m, 20H, $4C_6H_5$) ppm. ^{31}P NMR (81.0 MHz, $CDCl_3$, 85% H_3PO_4): 70.99 (s), 151.04 (s) ppm.

Preparation of (μ-*p*-MeC_6H_4S)(η^1-Ph_2PS-η^1)$Fe_2(CO)_6$ (9) and (μ-*p*-MeC_6H_4S)(η^1-Ph_2PS-η^1)$Fe_2(CO)_5$($Ph_2PC_6H_4Me$-*p*) (10). The same procedure was followed as for **7** and **8**, except that *p*-MeC_6H_4MgBr was used instead of EtMgBr. Elution with CH_2Cl_2/petroleum ether (1:6 v/v) afforded **9** as a red solid (0.397 g, 64%). Mp: 146−147 °C. Anal. Calcd for $C_{25}H_{17}Fe_2O_6PS_2$: C, 48.84; H, 2.76. Found: C, 48.69; H, 2.75. IR (KBr disk): $\nu_{C\equiv O}$ 2066 (vs), 2028 (vs), 1992 (vs), 1968 (vs) cm^{-1}. ^{1}H NMR (200 MHz, $CDCl_3$): 2.32 (s, 3H, CH_3), 7.07−7.80 (m, 14H, $2C_6H_5$, C_6H_4) ppm. ^{31}P NMR (81.0 MHz, $CDCl_3$, 85% H_3PO_4): 44.50 (s) ppm. From the second, bwown-red band **10** was obtained as a red solid (0.208 g, 24%). Mp: 127−128 °C. Anal. Calcd for $C_{43}H_{34}Fe_2O_5P_2S_2$: C, 59.45; H, 3.92. Found: C, 59.48; H, 4.06. IR (KBr disk): $\nu_{C\equiv O}$ 2040 (vs), 1974 (vs), 1947 (s), 1934 (s) cm^{-1}. ^{1}H NMR (200 MHz, $CDCl_3$): 2.20 (s, 3H, C*H*$_3C_6H_4P$), 2.39 (s, 3H, C*H*$_3C_6H_4S$), 6.73−7.72 (m, 28H, $4C_6H_5$, $2C_6H_4$) ppm. ^{31}P NMR (81.0 MHz, $CDCl_3$, 85% H_3PO_4): 57.99 (s), 70.41 (s) ppm.

Preparation of (η^1-Ph_2PS-η^1)$_2Fe_2(CO)_6$(11). To a stirred solution of (μ-S_2)$Fe_2(CO)_6$ (0.344 g, 1.0 mmol) in THF (20 mL) (cooled to −78 °C) was added a solution of Et_3BHLi (2 mL, 2 mmol) by syringe. At the midpoint of the addition, the solution turned from red to emerald green; for the rest of the addition it remained green. The green mixture was stirred at −78 °C for 15 min, and then Ph_2PCl (0.4 mL, 2.0 mmol) was added, causing an immediate color change back to red. The new mixture was allowed to warm to room temperature and stirred at this temperature for 1 h. The same workup as that for **7** and **8** gave **11** as a red solid (0.302 g, 42%). Mp: 132 °C (dec). Anal. Calcd for $C_{30}H_{20}Fe_2O_6P_2S_2$: C, 50.45; H, 2.82. Found: C, 50.72; H, 3.08. IR (KBr disk): $\nu_{C\equiv O}$ 2066 (vs), 2029 (vs), 2001 (vs), 1967 (s) cm^{-1}. ^{1}H NMR (200 MHz, $CDCl_3$): 7.25−8.07 (m, 20H, $4C_6H_5$) ppm. ^{31}P NMR (81.0 MHz, $CDCl_3$, 85% H_3PO_4): 49.71 (s) ppm.

Preparation of [(η^1-Ph_2PS-η^1)$Fe_2(CO)_6$]$_2$(4-μ-$SC_6H_4C_6H_4S$-μ-4′) (12). While stirring, a solution of 4-$BrC_6H_4C_6H_4Br$-4′ (0.312 g, 1.0 mmol) in THF (20 mL) was cooled to ca. −65 °C, and then a hexane solution of *n*-BuLi (ca. 2 mmol) was dropwise added to give an off-white mixture. The mixture was stirred for an additional 0.5 h from −65 to 0 °C and then recooled to −78 °C. To this mixture was added (μ-S_2)$Fe_2(CO)_6$ (0.688 g, 2.0 mmol), and after stirring for 15 min, Ph_2PCl (0.4 mL, 2.0 mmol) was added. The new mixture was stirred at −78 °C for 15 min and then allowed to warm to room temperature. After the mixture continued stirring at room temperature for 2 h, volatiles were removed and the residue was subjected to TLC separation using CH_2Cl_2/petroleum ether (1:2 v/v) as eluent. From the first, orange-red band **12** was obtained as a red solid (0.278 g, 23%). Mp: 145 °C (dec). Anal. Calcd for $C_{48}H_{28}Fe_4O_{12}P_2S_4$: C, 47.65; H, 2.33. Found: C, 47.64; H, 2.78. IR (KBr disk): $\nu_{C\equiv O}$ 2070 (vs), 2032 (vs), 2004 (vs), 1970 (s) cm^{-1}. ^{1}H NMR (200 MHz, $CDCl_3$): 7.33−7.85 (m, 28H, $4C_6H_5$, $2C_6H_4$) ppm. ^{31}P NMR (81.0 MHz, $CDCl_3$, 85% H_3PO_4): 44.69 (s) ppm.

Preparationof[(η^1-Ph_2PS-η^1)$Fe_2(CO)_6$]$_2$(4-μ-$SC_6H_4OCH_2CH_2$-OC_6H_4S-μ-4′) (13). The same procedure was followed as for **12**, except that 4-$BrC_6H_4OCH_2CH_2OC_6H_4Br$-4′ (0.372 g, 1.0 mmol) and excess *n*-BuLi (ca. 3 mmol) were used. From the first, orange-red band **13** was obtained as a red solid (0.523 g, 41%). Mp: 154 °C (dec). Anal. Calcd for $C_{50}H_{32}Fe_4O_{14}P_2S_4$: C, 47.24; H, 2.52. Found: C, 47.21; H, 2.55. IR (KBr disk): $\nu_{C\equiv O}$ 2069 (vs), 2031 (vs), 2003 (vs), 1985 (s), 1970 (s) cm^{-1}. ^{1}H NMR (200 MHz, $CDCl_3$): 4.28 (s, 4H, $2CH_2$), 6.84−7.83 (m, 28H, $4C_6H_5$, $2C_6H_4$) ppm. ^{31}P NMR (81.0 MHz, $CDCl_3$, 85% H_3PO_4): 67.02 (s) ppm.

Preparation of [(μ-MeS)$Fe_2(CO)_6$](μ_4-S)[(μ-Ph_2P)$Fe_2(CO)_6$] (14). A mixture of (μ-MeS)(η^1-Ph_2PS-η^1)$Fe_2(CO)_6$ (**1**, 0.181 g, 0.33 mmol) and $Fe_2(CO)_9$ (0.728 g, 2.0 mmol) in THF (20 mL) was stirred for 6 h at room temperature. After the solvent was removed under reduced pressure, the residue was subjected to TLC separation using CH_2Cl_2/petroleum ether (1:4 v/v) as eluent. From the major, orange-red band **14** was obtained as a red solid (0.069 g, 25%). Mp: 182 °C (dec). Anal. Calcd for $C_{25}H_{13}Fe_4O_{12}PS_2$: C, 36.41; H, 1.58. Found: C, 36.04; H, 1.70. IR (KBr disk): $\nu_{C\equiv O}$ 2078 (s), 2054 (vs), 2031 (vs), 1990 (vs), 1943 (s) cm^{-1}. ^{1}H NMR (200 MHz, $CDCl_3$): 2.07 (s, 3H, CH_3), 7.24−7.65 (m, 10H, $2C_6H_5$) ppm. ^{31}P NMR (81.0 MHz, $CDCl_3$, H_3PO_4): 145.63 (s) ppm.

Preparation of [(μ-PhS)$Fe_2(CO)_6$](μ_4-S)[(μ-Ph_2P)$Fe_2(CO)_6$] (15). The same procedure was followed as for **14**, except that (μ-PhS)(η^1-Ph_2PS-η^1)$Fe_2(CO)_6$ (**3**, 0.202 g, 0.33 mmol) was used instead of **1**. From the major band **15** was obtained as a red solid (0.032 g, 11%). Mp: 190−191 °C. Anal. Calcd for $C_{30}H_{15}Fe_4O_{12}PS_2$: C, 40.63; H, 1.69. Found: C, 40.42; H, 1.85. IR (KBr disk): $\nu_{C\equiv O}$ 2079 (s), 2052 (vs), 2030 (vs), 1994 (vs) cm^{-1}.

^{1}H NMR (200 MHz, $CDCl_3$): 7.19−7.74 (m, 15H, $3C_6H_5$) ppm. ^{31}P NMR (81.0 MHz, $CDCl_3$, 85% H_3PO_4): 145.53 (s) ppm.

Preparation of [(μ-EtS)$Fe_2(CO)_6$](μ$_4$-S)[(μ-Ph_2P)$Fe_2(CO)_6$] (16). The same procedure was followed as for **14**, except that (μ-EtS)(η^1-Ph_2PS-η^1)$Fe_2(CO)_6$ (**7**, 0.186 g, 0.33 mmol) was employed in place of **1**. From the major band **16** was obtained as a red solid (0.053 g, 19%). Mp: 173−174 °C. Anal. Calcd for $C_{26}H_{15}Fe_4O_{12}PS_2$: C, 37.23; H, 1.79. Found: C, 37.05; H, 2.24. IR (KBr disk): $\nu_{C\equiv O}$ 2078 (s), 2051 (vs), 2026 (vs), 1993 (vs), 1976 (vs), 1950 (m) cm^{-1}. ^{1}H NMR (200 MHz, $CDCl_3$): 1.33 (t, J = 7.2 Hz, 3H, CH_3), 2.41 (q, J = 7.2 Hz, 2H, CH_2), 7.31−7.70 (m, 10H, $2C_6H_5$) ppm. ^{31}P NMR (81.0 MHz, $CDCl_3$, 85% H_3PO_4): 145.78 (s) ppm.

Preparation of [(μ-Ph_2P)$Fe_2(CO)_6$(μ$_4$-S)$Fe_2(CO)_6$]$_2$(4-μ-SC_6H_4-C_6H_4S-μ-4′) (17). A solution of [(η^1-Ph_2PS-η^1)$Fe_2(CO)_6$]$_2$[4-μ-$SC_6H_4C_6H_4S$-μ-4′] (**12**, 0.204 g, 0.20 mmol) and $Fe_2(CO)_9$ (1.092 g, 3.0 mmol) in THF (20 mL) was stirred for 48 h at room temperature. After the solvent was removed under reduced pressure, the residue was subjected to TLC separation using THF/petroleum ether (1:5 v/v) as eluent. From the major, orange-red band **17** was obtained as a red solid (0.072 g, 20%). Mp: 90 °C (dec). Anal. Calcd for $C_{60}H_{28}Fe_8O_{24}P_2S_4$: C, 40.68; H, 1.58. Found: C, 40.81; H, 1.75. IR (KBr disk): $\nu_{C\equiv O}$ 2079 (s), 2053 (vs), 2031 (vs), 1994 (vs) cm^{-1}. ^{1}H NMR (200 MHz, $CDCl_3$): 7.32−7.80 (m, 28H, $4C_6H_5$, $2C_6H_4$) ppm. ^{31}P NMR (81.0 MHz, $CDCl_3$, 85% H_3PO_4): 145.51 (s) ppm.

Preparation of [(μ-Ph_2P)$Fe_2(CO)_6$(μ$_4$-S)$Fe_2(CO)_6$]$_2$(4-μ-SC_6H_4-OCH_2 $CH_2OC_6H_4S$-μ-4′) (18). The same procedure was followed as for **17**, but [(η^1-Ph_2PS-η^1)$Fe_2(CO)_6$]$_2$(4-μ-$SC_6H_4OCH_2CH_2OC_6H_4S$-μ-4′) (**13**, 0.254 g, 0.20 mmol) was used in place of **12**. Elution of the major, orange-red band with CH_2Cl_2/petroleum ether (5:1 v/v) produced **18** as a red solid (0.092 g, 25%). Mp: 85−87 °C. Anal. Calcd for $C_{62}H_{32}Fe_8O_{26}P_2S_4$: C, 40.66; H, 1.75. Found: C, 40.48; H, 1.88. IR (KBr disk): $\nu_{C\equiv O}$ 2079 (s), 2052 (vs), 2030 (vs), 1994 (vs) cm^{-1}. ^{1}H NMR (200 MHz, $CDCl_3$): 4.20 (s, 4H, $2CH_2$), 6.70, 6.74, 7.13, 7.17 (AB quartet, 8H, $2C_6H_4$), 7.30−7.67 (m, 20H, $4C_6H_5$) ppm. ^{31}P NMR (81.0 MHz, $CDCl_3$, 85% H_3PO_4): 145.60 (s) ppm.

X-ray Structure Determinations of 9, 11, and 14. Single crystals of **9**, **11**, and **14** suitable for X-ray diffraction analyses were grown by slow evaporation of a hexane solution of **9** and a hexane/CH_2Cl_2 solution of **14** at about 4 °C, and by slow diffusion of hexane into a diethyl ether solution of **11** at about 4 °C, respectively. A single crystal of **9**, **11**, or **14** was mounted on a Bruker SMART 1000 automated diffractometer. Data were collected at room temperature, using a graphite monochromator with Mo Kα radiation (λ = 0.71073 Å) in the $\omega-\phi$ scanning mode. Absorption correction was performed by the SADABS program.[40] The structures were solved by direct methods using the SHELXS-97 program[41] and refined by full-matrix least-squares techniques (SHELXL-97)[42] on F^2. Hydrogen atoms were located by using the geometric method. Details of crystal data, data collections, and structure refinements are summarized in Table 2.

Electrochemistry. Acetonitrile (Fisher Chemicals, HPLC grade) was used for electrochemistry assays. A solution of 0.1 M n-Bu_4NPF_6 in MeCN was used as electrolyte in all cyclic voltammetric experiments. Electrochemical measurements were made using a BAS Epsilon potentiostat. All voltammograms were obtained in a three-electrode cell with a 3 mm diameter glassy carbon working electrode, a platinum counter electrode, and an Ag/Ag$^+$ (0.01 M $AgNO_3$/0.1 M n-Bu_4NPF_6 in MeCN) reference electrode under N_2 atmosphere. The working electrode was polished with 0.05 μm alumina paste and sonicated in water for at least 10 min prior to use. Bulk electrolysis was run on a vitreous carbon rod (ca. 3 cm^2) in a two-compartment, gastight, H-type electrolysis cell containing ca. 20 mL of MeCN. All potentials are quoted against the ferrocene/ferrocenium (Fc/Fc$^+$) potential. Gas chromatography was performed with a Shimadzu GC-9A gas chromatograph under isothermal conditions with nitrogen as a carrier gas and a thermal conductivity detector.

Acknowledgment. We are grateful to the National Natural Science Foundation of China and the Research Fund for the Doctoral Program of Higher Education of China for financial support.

Supporting Information Available: Full tables of crystal data, atomic coordinates and thermal parameters, and bond lengths and angles for **9**, **11**, and **14** as CIF files. This material is available free of charge via the Internet at http://pubs. acs.org.

OM800077C

---

(40) Sheldrick, G. M. *SADABS, A Program for Empirical Absorption Correction of Area Detector Data*; University of Göttingen: Germany, 1996.

(41) Sheldrick, G. M. *SHELXS97, A Program for Crystal Structure Solution*; University of Göttingen: Germany, 1997.

(42) Sheldrick, G. M. *SHELXL97, A Program for Crystal Structure Refinement*; University of Göttingen: Germany, 1997.